UNPUBLISHED PRELIMINARY DATA

PERSTARE ET PRAESTARE MDCCCXXXIX

NEW YORK UNIVERSITY

School of Engineering and Science

RESEARCH DIVISION

University Heights, Bronx 53, N. Y.

Department of Meteorology and Oceanography

Geophysical Sciences Laboratory Report No. 65-1

RADIATION STUDIES FROM METEOROLOGICAL SATELLITES

by

S. I. Rasool

and

C. Prabhakara

January 1965

New York University
School of Engineering and Science
Research Division
Department of Meteorology and Oceanography
Geophysical Sciences Laboratory Report 65-1

RADIATION STUDIES FROM METEOROLOGICAL SATELLITES

by

S. I. Rasool
Department of Meteorology and Oceanography
New York University

and

C. Prabhakara
Goddard Institute for Space Studies
National Aeronautics and Space Administration

A report of Project Hiam. The research reported here was supported in part by Grant No. NS G-499 from the National Aeronautics and Space Administration and in part by the Goddard Institute for Space Studies. Part of the work was done while Dr. Rasool was a National Academy of Sciences-National Research Council Senior Research Associate at the Goddard Institute for Space Studies.

January 1965

Errata

Change 26% to 30% on line 8 of abstract and p 4, l. 13. - NASA Technical Evaluator per S.I.R. 5/28/65

CONTENTS

LIST OF FIGURES

Abstract

22552.

Analysis has been made of the radiation measurements made by the Tiros meteorological satellites during 1962 and 1963. Data for 10 months have been analyzed to obtain information on the latitudinal and time variations of the albedo of the earth and the outgoing terrestrial radiation in the infrared.

The albedo values thus obtained give a mean reflectivity of the earth-atmosphere system of 31 percent for the area between the latitudes 60°N and 60°S. The oceanic regions contribute [redacted] percent while the land areas, 34 percent. A conspicuously high albedo of ~45 percent is noted over the desert regions of the Sahara and Arabia which implies a slightly negative radiative balance of these regions.

The latitudinal and monthly variation in the total outgoing radiation indicates a substantially high radiation being emitted in August, September and October from the subtropical belts in both the hemispheres.

The albedo values are used to derive the effective incoming radiation from the sun which is then combined with the estimates of the outgoing radiation in the infrared to obtain monthly mean radiative energy balance of the earth-atmosphere system for each 10° latitude belt between 60°N and 60°S.

An attempt is then made to derive, from these data, the energy available for transport by the atmosphere and oceans. For this purpose we algebraically add to the radiation balance obtained from Tiros the two other important parameters, viz., storage of energy by oceans, land and atmosphere, and the net latent heat. The heat stored in the oceans for each month and for each 10° latitudinal belt is deduced from the climatological estimates of the variations in the ocean temperatures around the globe. The net latent heat released in the atmosphere is calculated from the climatological estimates of precipitation and evaporation.

The sum of these three energy terms, viz., the radiation balance, the storage and the net latent heat results in the estimates of heat which is available, at each latitudinal belt, for meridional transportation by oceans and by the atmosphere. The energy distribution patterns indicate that ocean transport may be much more significant in the southern hemisphere than in the northern hemisphere, particularly during the months of February through May.

Author

1. Background

Solar energy, the primary source for driving the atmospheric heat engine, has a flux of 1.4×10^6 ergs cm^{-2} sec^{-1} or 2 calories cm^{-2} min^{-1} at the top of the earth's atmosphere. Part of this radiation is reflected back to space mainly by the clouds. The albedo of the earth has been estimated by various authors and the values range between 35 and 40 percent (Danjon, 1936; Fritz, 1949; Angström, 1963). The remaining 60 to 65 percent of the solar energy is absorbed in the atmosphere and at the surface of the earth.

The earth-atmosphere system radiates back to space in the far infrared. Over long periods of time, of the order of years, the total amount of radiation thus emitted back to space equals the total incoming solar radiation. This long period global radiative balance may be expressed as follows:

$$\frac{S.C.}{4}(1 - A) = E_s = E_r = \sigma T_e^4 \qquad (1)$$

where S. C. is the solar constant at the distance of the earth (2 cal cm^{-2} min^{-1}), A is the average albedo of the whole globe, E_s is the effective incoming solar radiation, E_r is the total outgoing radiation from the earth-atmosphere system in the far infrared, T_e is the effective temperature of the earth, and σ is the Stefan-Boltzmann constant.

Over a short period of time, and for any given region of the globe, however, the difference between the incoming and outgoing radiation ($E_s - E_r$), known as the local radiation balance of the

earth-atmosphere system, is not necessarily zero and may be a finite quantity. This radiation balance, R, varies with latitude, longitude, and season and is generally known to be positive near the equator and negative at the poles (Simpson, 1929; Houghton, 1954; London, 1957).

The radiation imbalance ($R \neq 0$) over a given region may manifest itself in three different ways: (1) by a change in the combined heat content of the oceans or land and of the atmosphere; (2) by an increase or decrease of the latent heat; and (3) by transport of energy by ocean and air currents from or to this region. The following equation expresses the local heat balance of the earth-atmosphere system:

$$R = S + LE + T \qquad (2)$$

where S is the storage of energy which itself has three components: S_O, S_L, S_A, being the storage in oceans, land, and the atmosphere. Of these, the storage in the oceans is the most significant, and can have an approximate magnitude of the radiation balance itself (Gabites, 1950; Fritz, 1958). S_L and S_A are usually 10 percent of S_O (Gabites, 1950). LE is the net latent heat available in the atmosphere, being the difference between the amount of energy spent in evaporation and that released by condensation in the atmosphere. T is the transport of heat by ocean currents and by winds.

Studies on the radiation balance of the earth-atmosphere system date back to 1929 when Simpson, for the first time, derived a geographical distribution of the radiative energy balance over the whole globe for different seasons. He concluded that the globe as a whole is in radiative equilibrium and showed a large positive radiation balance over desert regions in summer. These findings have been reexamined in recent

years by Gabites (1950), Houghton (1954), Budyko (1956), London (1957), Fritz (1958), Davis (1963), and others. Of these, Gabites (1950) and Fritz (1958) investigated the problem of ocean storage in great detail and were able to compute the net amount of heat available in the atmosphere for transport across latitudes: a parameter significant in the study of general circulation.

The studies cited above were based on the ground observations of the incoming solar radiation and on the theoretical estimates of the outgoing radiation in the infrared. These two parameters in the studies of heat balance are the most important and now, with the advent of meteorological satellites, we are in a position to reexamine this question with much more extensive coverage of the globe and a frequency of observation never before achieved.

2. Radiation experiments by meteorological satellites

Explorer VII, launched in 1959, was the first satellite to carry an experiment of meteorological significance (Suomi, 1958, 1961). The instrumentation consisted of white and black hemispheric sensors. The black hemispheres responded to both the short wave solar radiation reflected by the earth and to the long wave terrestrial radiation, while white sensors are only sensitive to the far infrared radiation. By combining the measurements made by the two sensors, an estimate of the reflected solar energy and the outgoing terrestrial radiation can be obtained.

Though the orbit of Explorer VII covered the major part of the globe, viz. 50°N to 50°S, the satellite was not equipped for storing the

data, and radiation measurements were only available in the vicinity of the interrogating stations. Despite this disadvantage, several months of exploitable data were accumulated over different regions of the globe, and have been the subject of a series of studies on the distribution of the outgoing terrestrial radiation over the globe (Suomi, 1961). The principal findings from these measurements confirmed the hitherto expected and theoretically calculated results that the regions of high pressure, which are usually cloudfree, emit large amounts of far infrared radiation to space.

Major improvements in the radiation instrumentation were incorporated in Tiros II, launched on November 23, 1960, and in the subsequent Tiros series of satellites. Tiros II, III, IV, and VII contained, in addition to the Explorer-type instrument, a medium resolution scanning radiometer. These radiometers have been described in considerable detail by Bandeen et al. (1961) and by Astheimer et al. (1961). The radiometers measure the absolute intensities of the emitted terrestrial radiation and of the solar radiation as reflected by the earth. These measurements are made in five selected narrow spectral intervals in the visible and in the far infrared. Figure 1 shows the spectral response of the three infrared channels of the Tiros radiometer as a function of wavelength. In the same figure, the dotted curve shows the percentage transmissivity of the earth's atmosphere in the far infrared.

The spectral intervals in the infrared to which individual channels respond have been so selected as to give information regarding the temperatures in different regions of the atmosphere. The channel responding to the energy in the 6 to 6.5 μ interval is centered in the

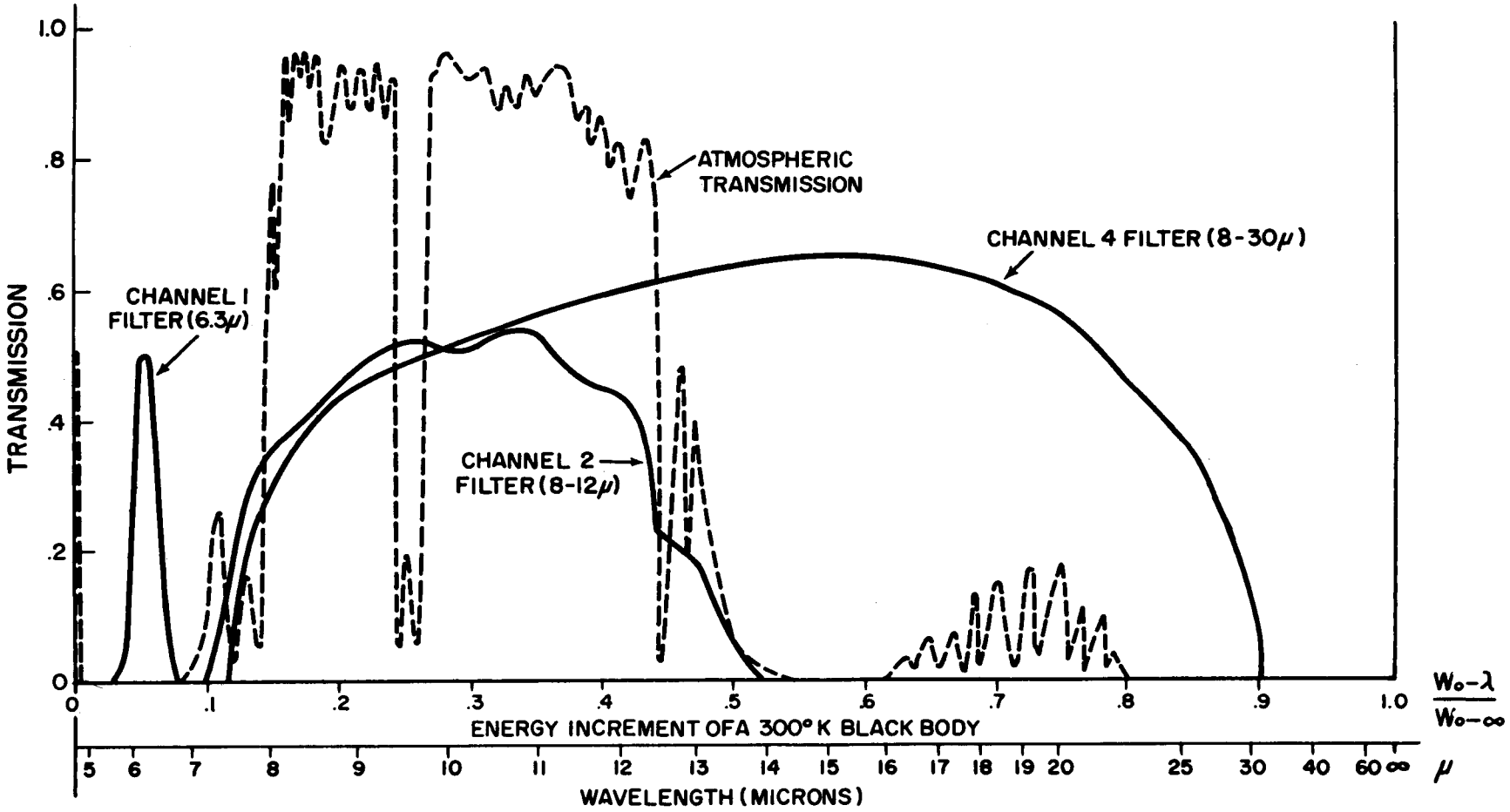

Figure 1. Filter transmission characteristics of channels 1, 2, and 4 of the medium resolution radiometer. The dashed line is the approximate transmission characteristic of the earth's atmosphere. (After Bandeen et al., 1961)

spectral region where water vapor has a strong absorption band. This channel therefore records emission only from the upper troposphere. On the other hand, in the 8 to 12 μ spectral interval, the atmosphere is largely transparent. The satellite radiometer "looking" in this spectral interval (Channel 2) records energy emitted from very near the ground. The third infrared channel, measuring energy in the 7 to 30 μ interval, records approximately 80 percent of the total radiation emitted by the earth and the atmosphere and can therefore be used in the study of the total outgoing terrestrial radiation.

Clouds are usually assumed to be completely opaque to wavelengths longer than 3μ. In the presence of clouds, therefore, both the radiometric channels measuring radiation in the 8 to 12 μ and 7 to 30 μ intervals record energy radiated by the atmosphere from above the cloud tops.

For the measurement of reflected solar radiation in the visible and near infrared, the Tiros radiometer is equipped with two other channels, the first sensitive in the 0.5 to 0.7 μ wavelength interval and the other in the 0.2 to 5 μ interval. Measurements in these channels can be used to derive information on the albedo of the earth and consequently on the amount of solar radiation absorbed by the earth-atmosphere system.

Recent analyses of the radiation data obtained from Tiros have indicated that there has been considerable degradation in the instrumental response, thereby introducing an error in the observed radiation values. Because the Tiros satellites do not have on-board calibration facilities, the corrections to these degradations have to be determined indirectly. Bandeen (private communication) has studied this problem in great

detail and has communicated the correction factors for individual channels in each one of the satellites. These corrections are based on the assumption that the quasi-global (60°N to 60°S) mean values of the radiation reflected in the short wave and emitted in the long wave regions remain constant over long periods of time (several months).

2.1 Orbital characteristics

The inclination of the orbits of Tiros II, III, and IV was 48° and that of Tiros VII, 58°. Coverage of the globe is therefore limited, in the first three satellites, to about 55°N and S, and in the case of Tiros VII, to 65°N and S.

The Tiros satellites are spin-stabilized which implies that the direction of the spin axis remains fixed in space. The five-channel radiometer is installed in the satellites at an angle of 45° to the spin axis and has a field of view of a 5° cone. This field of view corresponds to an area on the surface of the earth of 60 x 60 km when the radiometer is viewing vertically down. Because the spin axis is fixed in space, there is a limitation on the coverage of the data for the periods of the orbits when the radiometer is not looking at the earth. Figure 2 shows the scan pattern of the Tiros radiometer.

The interrogating stations were, until now, situated only in the United States, and since the satellite has a capacity to store data for only one orbit, the data for three of the fourteen orbits each day is lost. Also, the orbit of the satellite precesses in right ascension at the rate of about $6° \text{ day}^{-1}$. For this reason, the measurements of the reflected solar radiation may be confined to only one hemisphere for a period of time of the order of several weeks. However, in nine weeks, the

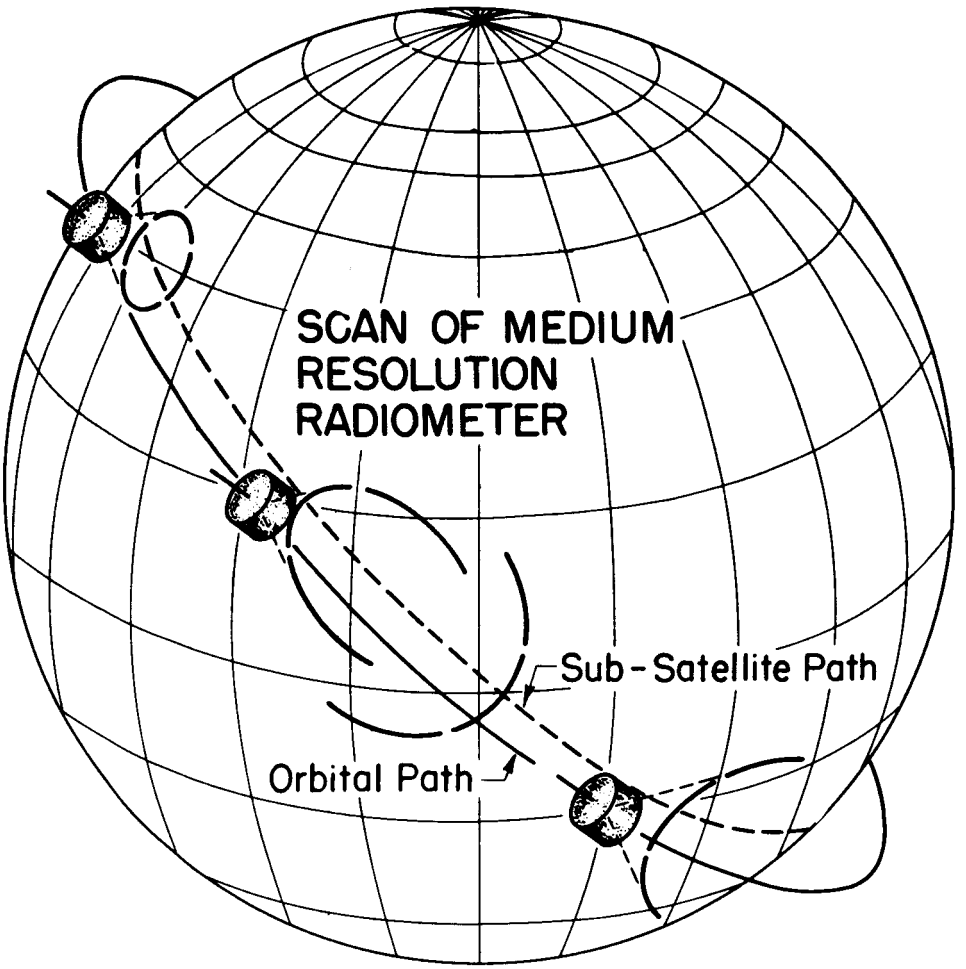

Figure 2. Geometry of the scanning motion of the medium resolution radiometer and of the viewing area of the low resolution radiometer. (After Bandeen et al., 1961.)

precession cycle around the globe is completed and the visible channels can cover the whole globe.

2.2 Albedo measurements from satellites

Two of the five channels of the Tiros radiometers are sensitive in the spectral range 0.2 to 5 μ and 0.5 to 0.75 μ, respectively. The amount of energy measured by the radiometer in each channel yields the fraction of the solar radiation, in the corresponding spectral interval, reflected back to space in the direction of the satellite by the earth-atmosphere system. The measurements of the reflected energy in the 0.2 to 5 μ channel, which covers practically the entire solar spectrum, are used in the present study to derive the albedo, A, by the following expression:

$$A = \frac{\text{reflected energy measured in } 0.2 \text{ to } 5\mu}{(\text{total solar energy in } 0.2 \text{ to } 5\mu)\cos z} \qquad (3)$$

where z is the zenith angle of the sun at the time and point of observation. Only those measurements are included for which the solar zenith angle was less than 60° and the satellite nadir angle (angle between the line of view of the radiometer and the local radius vector of earth) less than 45°. It is also assumed that the scattering of the solar radiation by the earth's surface and by the atmosphere is isotropic. This assumption may not be valid at high phase angles (Arking, 1964) and the values derived here may eventually require small corrections.

The individual albedo values thus calculated were averaged in the region of 5° latitude by 5° longitude grids for the period February through June 1962. In Figure 3 we show the global distribution of the albedo thus deduced from the measurements made by Tiros IV. The

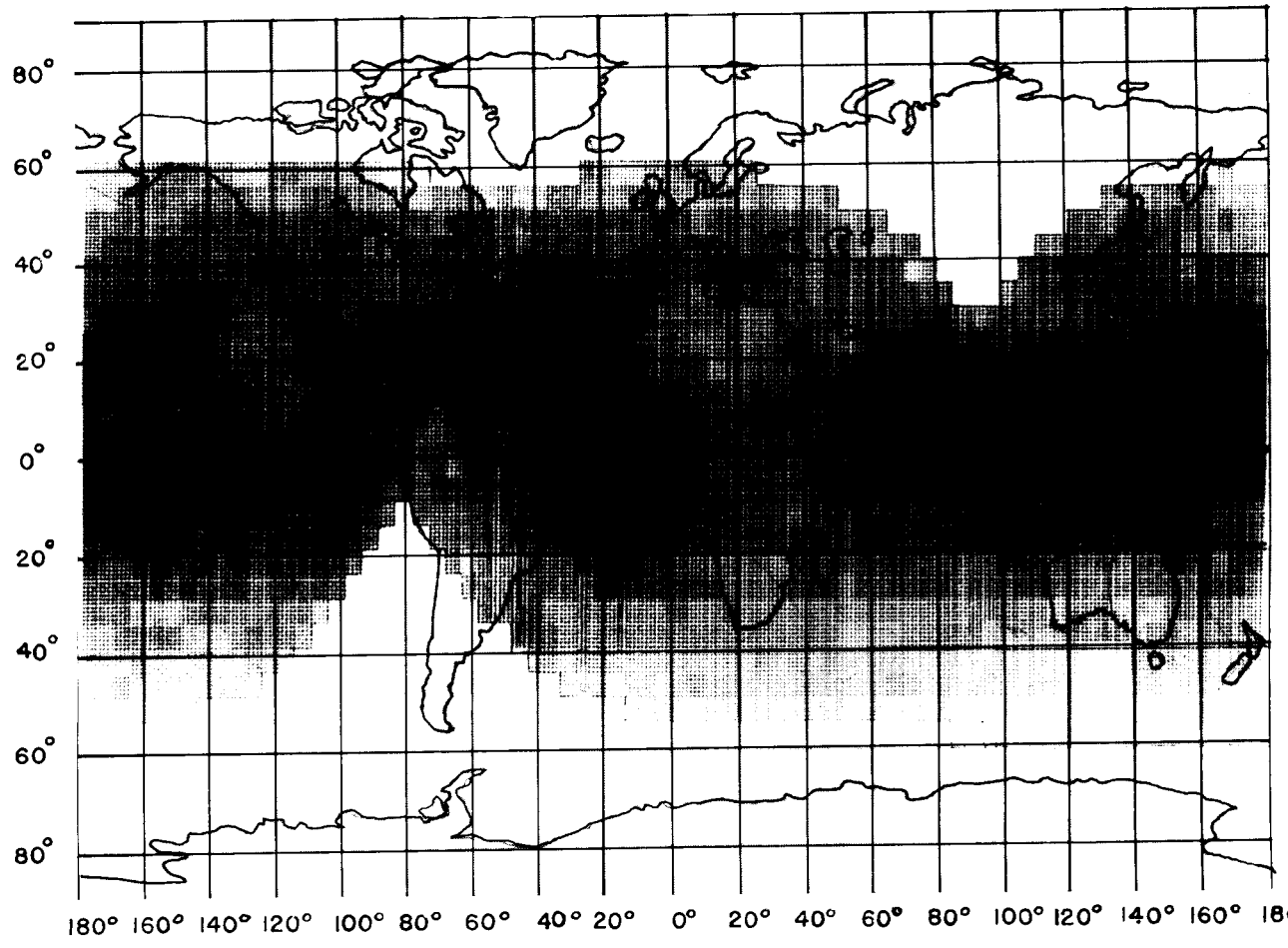

Figure 3. Global distribution of the albedo of the earth-atmosphere system, February through June 1962 (Tiros IV). Six shades in steps of 10%, ranging from minimum value (0 - 10%) represented as the darkest shade, e. g., central Atlantic, to maximum value (50 - 60%) shown as the lightest shade, e. g., at 50°S.

two triangular regions comprising parts of South America and Central Asia have been left blank because data are not available for these areas. There are about 500 observation points in each 5° by 5° grid, and only those grids which had more than 100 readings have been included in this figure. The albedo values shown in Figure 3 are in steps of 10 percent, ranging from a value of less than 10 percent (darkest shade) to 60 percent (lightest shade).

An examination of Figure 3 shows the following interesting features:

(1) The oceanic regions, especially in the subtropics, show albedo of the order of only 20 percent. The albedo of the land areas is considerably higher, of the order of 30 to 40 percent. On an average, the albedo of the oceans is 30 percent while that of the land areas is 34 percent. The mean reflectivity of the earth-atmosphere system, between latitudes 60°N and 60°S, is 31 percent.

(2) The patterns of albedo appear to follow the continental boundaries and strong gradients of albedo are observed at the coast lines. In the southern hemisphere, which is mostly oceanic, the albedo values do not show much longitudinal variation, except in the case of the subtropical belt where we notice, as an almost permanent feature, three regions of low albedo situated over the three oceans.

(3) The Sahara and Arabian deserts show a conspicuously high albedo, about 45 percent, for this five month period. This value is comparable with the albedos measured over Central Africa and South Americs which are regions of high cloudiness. More detailed examination of the albedo values recorded over these desert regions for

individual months show persistently high values.

These results are also supported by measurements made by Tiros III for which good data for the visible channels are available only for a 10-day period between July 12 and July 21, 1961.

We have also analyzed the visible channel data from Tiros VII corresponding to the period of June through November 1963. Again the absolute values are uncertain due to the instrumental degradation noticed for this satellite also, but after applying an appropriate degradation correction, we find relatively high values over the Sahara for this period also. The average albedo for the five month period over the Sahara is, in this case, 40 percent. These results suggest that the deserts of North Africa and Arabia have an average albedo of 40 to 45 percent throughout the year.

This result, the high albedo of deserts, implies that the amount of solar radiation actually absorbed by the land and the atmosphere in these regions may be considerably less than hitherto believed. A comparison of the value of incoming solar radiation with the amount of infrared radiation emitted by these regions, as measured by the same satellite, indicates that the radiative balance of the land-atmosphere system for the Sahara may be zero or even slightly negative. This result is in contradiction with the earlier published results which were based on the assumption that the albedo of the Sahara is about 20 to 25 percent (Buettner, 1929), giving a positive energy balance over the region (Simpson, 1929; Budyko, 1956; Rasool, 1964).

In a recent study on the climate of the Sahara, Dubief (1959) reports an albedo value of as high as 44 percent measured by Failletaz

over selected regions of the desert. Dubief also suggests that large sandy areas may have still higher albedo. Results from Tiros seem to be consistent with the measurements of Failletaz.

3. Radiative energy balance

The chief objective of this analysis is to use the radiation data acquired by Tiros satellites to derive time and latitudinal variations of the radiation balance of the earth-atmosphere system. The radiation balance is made up of the difference between the incoming solar radiation and the outgoing terrestrial radiation in the infrared.

3.1 Incoming solar radiation

With the combination of the albedo data from Tiros IV, February 8 to June 30, 1962 and from Tiros VII, June 19 to November 20, 1963, we are now in a position to calculate the incoming radiation for the 10-month period of February through November. However, in matching the data from two separate years, it is found that the albedos for the month of June in 1962 and 1963 agree with one another within 5 percent. So we have adopted the data of February 12 to June 30, from 1962 and July 1 to November 20 from 1963 to get the total 10-month period.

The incoming radiation, E_s, in a given 10° latitudinal belt for each month, is calculated from the expression:

$$E_s = E(1 - \bar{A}) \tag{4}$$

where E is the average radiation flux incident at the top of the atmosphere for the month and $\bar{A}$ is the monthly mean albedo for the latitudinal belt.

Figure 4 shows the distribution of the incoming solar radiation as a function of latitude and month between 60°N and 60°S in cal cm^{-2} day^{-1}.

The middle and subtropical latitudes in the northern hemisphere receive conspicuously high radiation in the months of June and July. It may be noted that the subtropical latitudinal belt in the southern hemisphere receives more radiation in the local summer than in the northern hemisphere. This is both because of the large oceanic regions in this hemisphere, which have a relatively low albedo as shown in Figure 3, and also because of slightly more solar radiation incident at the top of the atmosphere over the southern hemisphere summer.

3.2 Outgoing terrestrial radiation

The other component of the radiation balance is the outgoing terrestrial radiation in the far infrared. Tiros data has so far been used by several authors to determine the latitudinal distribution of outgoing radiation for specific periods (Winston and Rao, 1962; Prabhakara and Rasool, 1963; Nordberg et al., 1962; House, 1964). The values in the northern hemisphere derived from these measurements have been fairly consistent with the earlier estimates made by London (1957). Now with the availability of data from Tiros IV and VII, and applying the degradation corrections communicated by Bandeen, we calculate the total outgoing radiation for each 10° latitudinal belt for 10 individual months, February through June 1962 and July through November 1963. Figure 5 shows the latitudinal and time variations of the total outgoing radiation in cal cm^{-2} day^{-1}.

The variation in the outgoing radiation with latitude is small

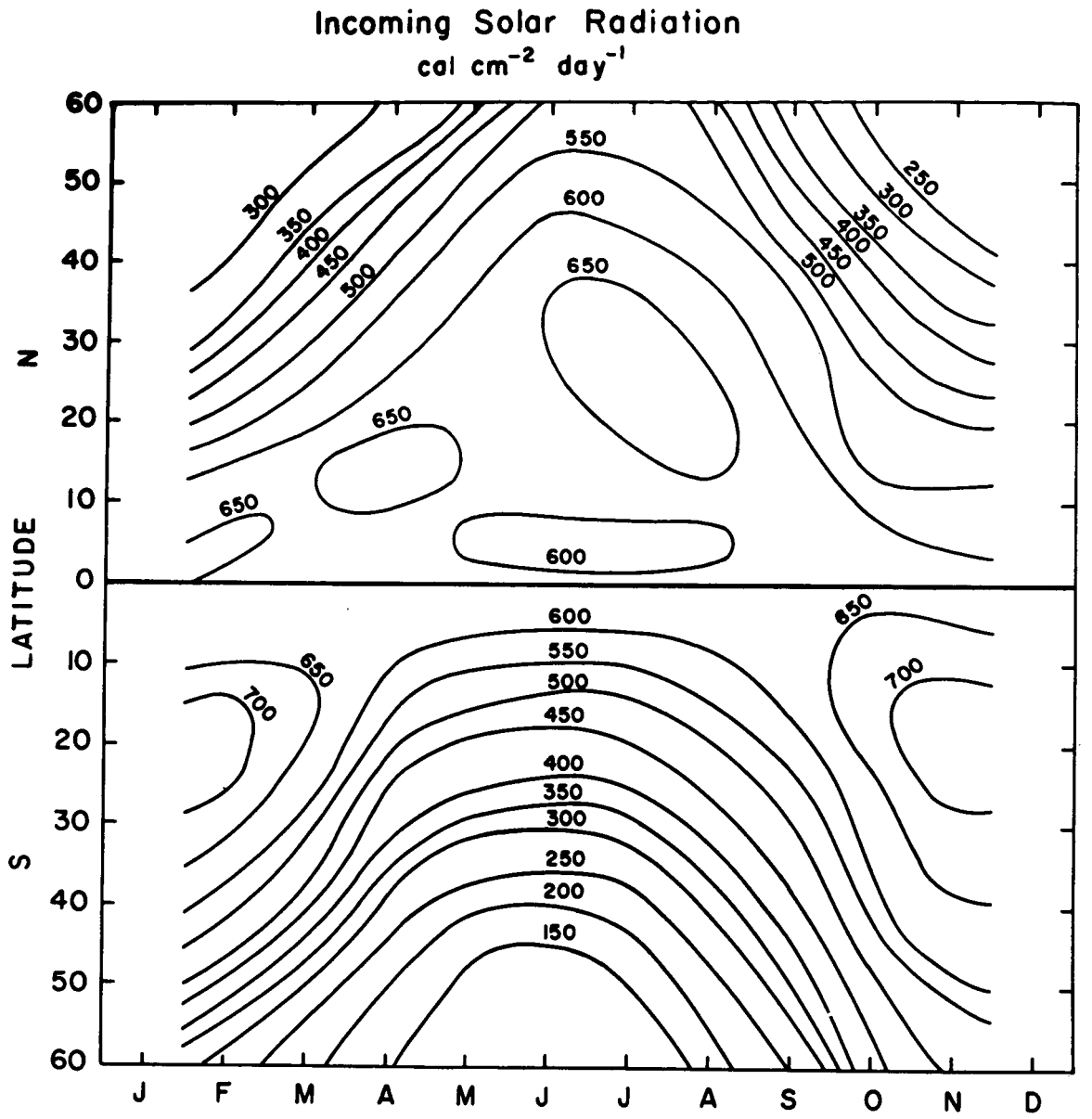

Figure 4. Latitude and time distribution of the incoming solar radiation in cal cm^{-2} day^{-1} derived from the albedo measurements made by Tiros IV and VII.

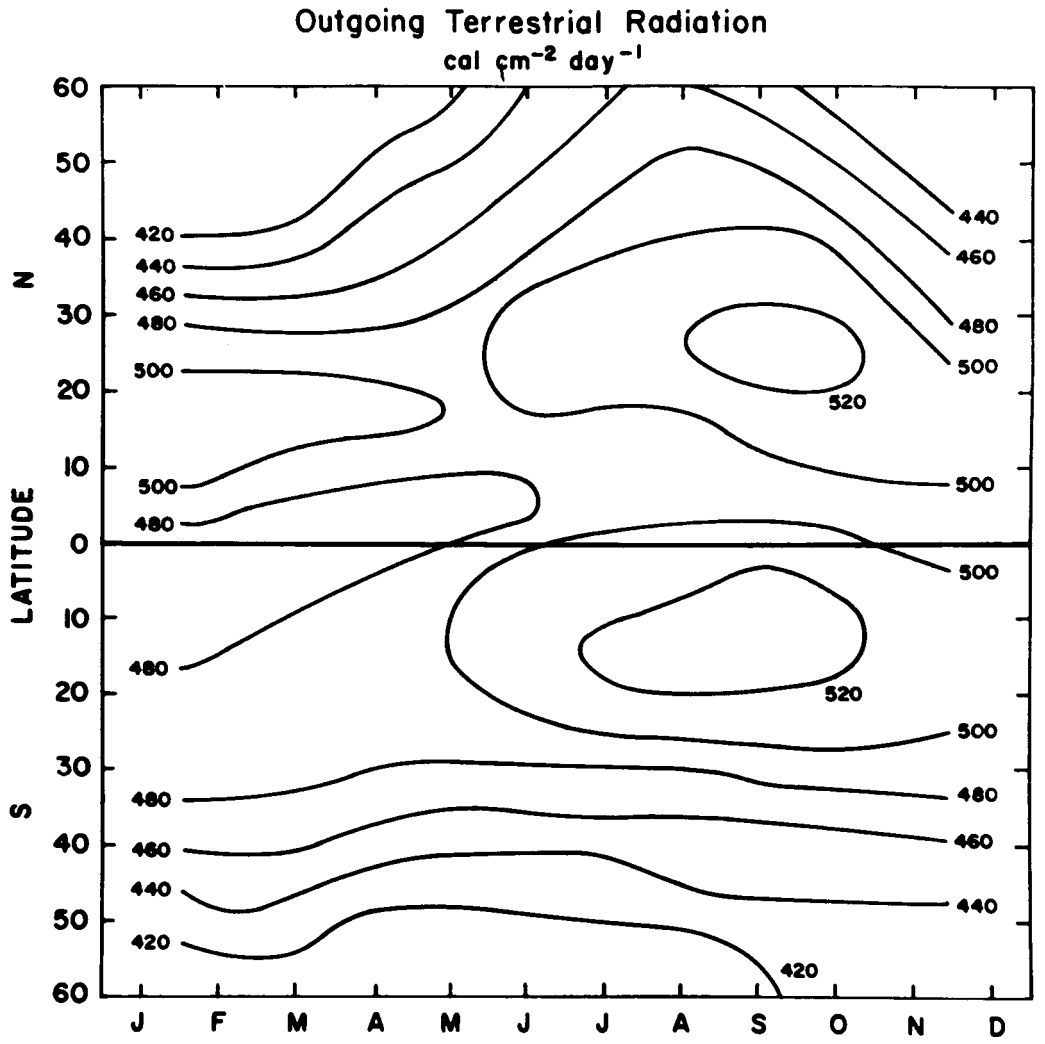

Figure 5. Latitude and time distribution of the outgoing terrestrial radiation in the far infrared in cal cm^{-2} day^{-1} derived from measurements made by Tiros IV and VII.

and the change with season is still smaller. The two weak highs of outgoing radiation situated on either side of the equator are noted. They both occur in the months of August, September and October, although the seasons are opposite in the two hemispheres. Also the latitude of the intertropical convergence zone (region of the equatorial minimum in the outgoing radiation) changes as expected from 5°S in February to about 5°N in July and August.

3.3 Energy balance of the earth-atmosphere system.

Combining Figures 4 and 5, we now obtain the radiation balance of the earth-atmosphere system shown in Figure 6. Because the total outgoing terrestrial radiation does not vary considerably with season and with latitude between 60°N and 60°S, the radiation balance of the earth-atmosphere system shows a pattern similar to that of the incoming radiation (Fig. 5). The main excess of incoming over outgoing radiation occurs in the latitudes 20 to 40° in both hemispheres in the respective months of summer. In the tropical latitudes between 20°N and 15°S, there is an excess of incoming radiation all year round.

The radiation balance as shown in Figure 6 gives the net amount of energy deposited by the sun in the earth-atmosphere system. It is well known, however, that a substantial part of this energy is stored in the oceans and to some extent also in the land and atmosphere. Also part of this energy is spent in evaporation of water which may later be released in the atmosphere by condensation in the form of clouds. The remaining part is termed the energy available for transportation across the latitudinal circles, both by the atmosphere and the oceans. We shall now attempt to evaluate the magnitude of energy involved in each

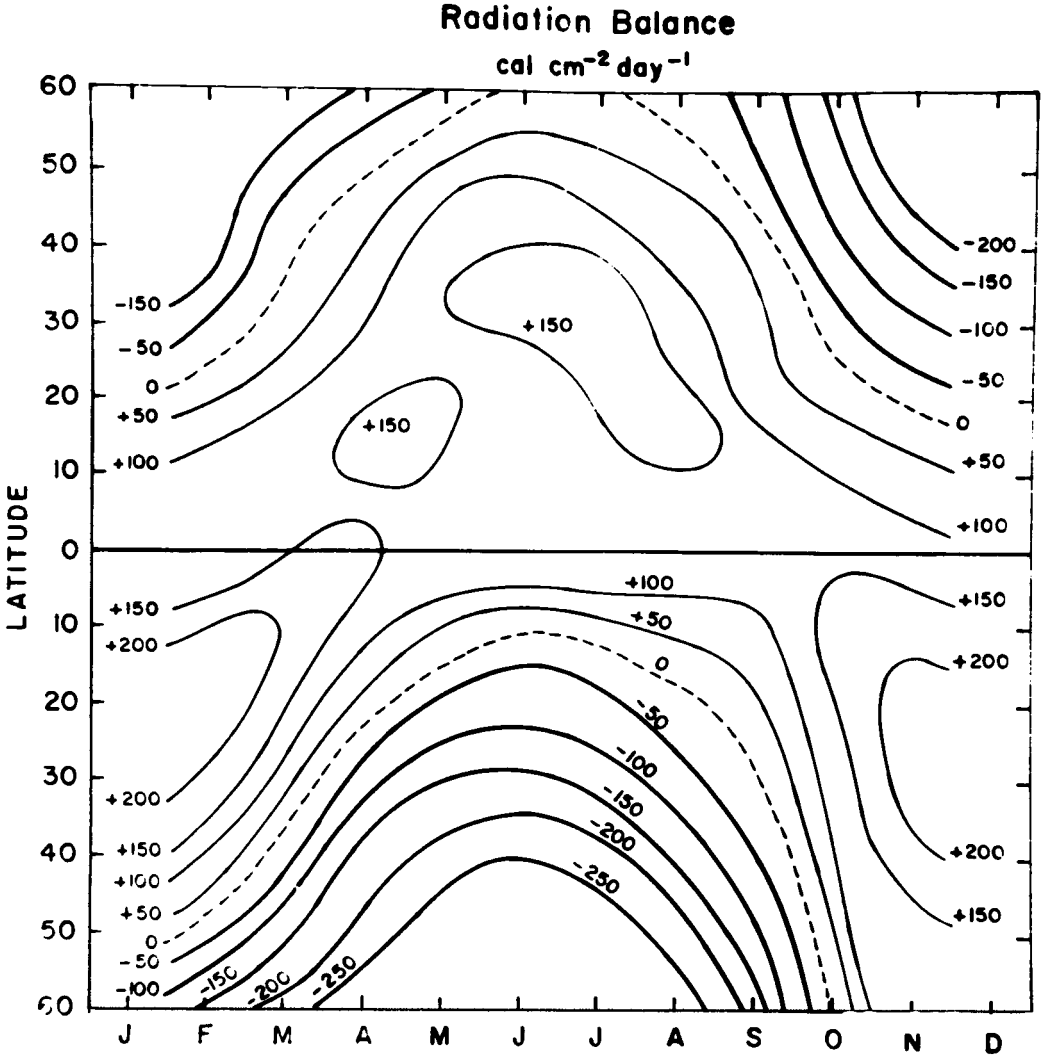

Figure 6. Radiation balance of the earth-atmosphere system in cal cm^{-2} sec^{-1} derived from Figures 4 and 5.

of these processes.

4. Heat storage

4.1 Storage in oceans

The first comprehensive study of heat storage in the oceans, both as a function of season and latitude, was made by Gabites (1950). The heat storage in the oceans was calculated, on a monthly basis, from the observed temperature increase in the first 100 m below the ocean surface. Gabites adopted an equivalent thickness of 75 m depth which supposedly will be uniformly heated or cooled for a given change in surface temperature. He thus calculated that a change of 1 °C in the surface temperature of the ocean will correspond to a change of heat storage of the ocean by 7500 cal. Fritz (1958), however, pointed out that there is considerable phase lag in the variation of ocean temperatures with depth, and taking this into account reevaluated the heat storage in oceans. Using the more recent bathythermograph data analysis for the region of 20 °N to 20 °S and 120 °W to 160 °W (East Pacific), Fritz derived empirical relations to convert the change in ocean surface temperature to the heat storage for each individual month. From the observed surface temperatures over all the oceans of the northern hemisphere, Fritz deduced the latitudinal variations of the amount of heat storage in each month for the northern hemisphere. These results were significantly different from those derived earlier by Gabites, especially for middle latitudes. More recently, Shroeder and Bryan (1960) have studied the heat storage in the Atlantic on an annual basis and their results agree with those of Fritz for the respective latitudinal belts.

For our computations of storage of heat in oceans, we have adopted the following procedure: The monthly mean surface temperatures in the Atlantic, Pacific, and Indian Oceans are collected from the United States Marine Climatic Atlas (1955), and are averaged for every 10° latitudinal belt between 60°N and 60°S. In order to convert the monthly changes in surface temperature into the amount of heat stored, we adopt the conversion factors published by Fritz for the latitudinal belts between 20°N and 60°N. For 20°S to 60°S, we use the same empirical relations, assuming that they also are valid for the southern hemisphere with a time difference of six months. For the equatorial regions (20°N to 20°S), however, we assume that only one conversion factor is valid for all the 12 months, and it is derived by averaging Fritz' values for the whole year. It is observed that the variations in the monthly mean ocean surface temperatures in the equatorial regions are very small (of the order of 1/5 of the variation in middle latitudes) and any error which may result from this assumption will probably be small. The amount of storage is then weighted according to the fractional area of oceans in each latitudinal belt to obtain the ocean heat storage as shown in Figure 7. These values compare very well with those published by Fritz, even though we have used more recent data on the surface temperature variations in the ocean. In spite of the large percentage cover of oceans in the southern hemisphere, the amount of heat stored is comparable to that in the northern hemisphere. This could be due to smaller changes in the surface temperature in the southern hemisphere compared to the northern hemisphere.

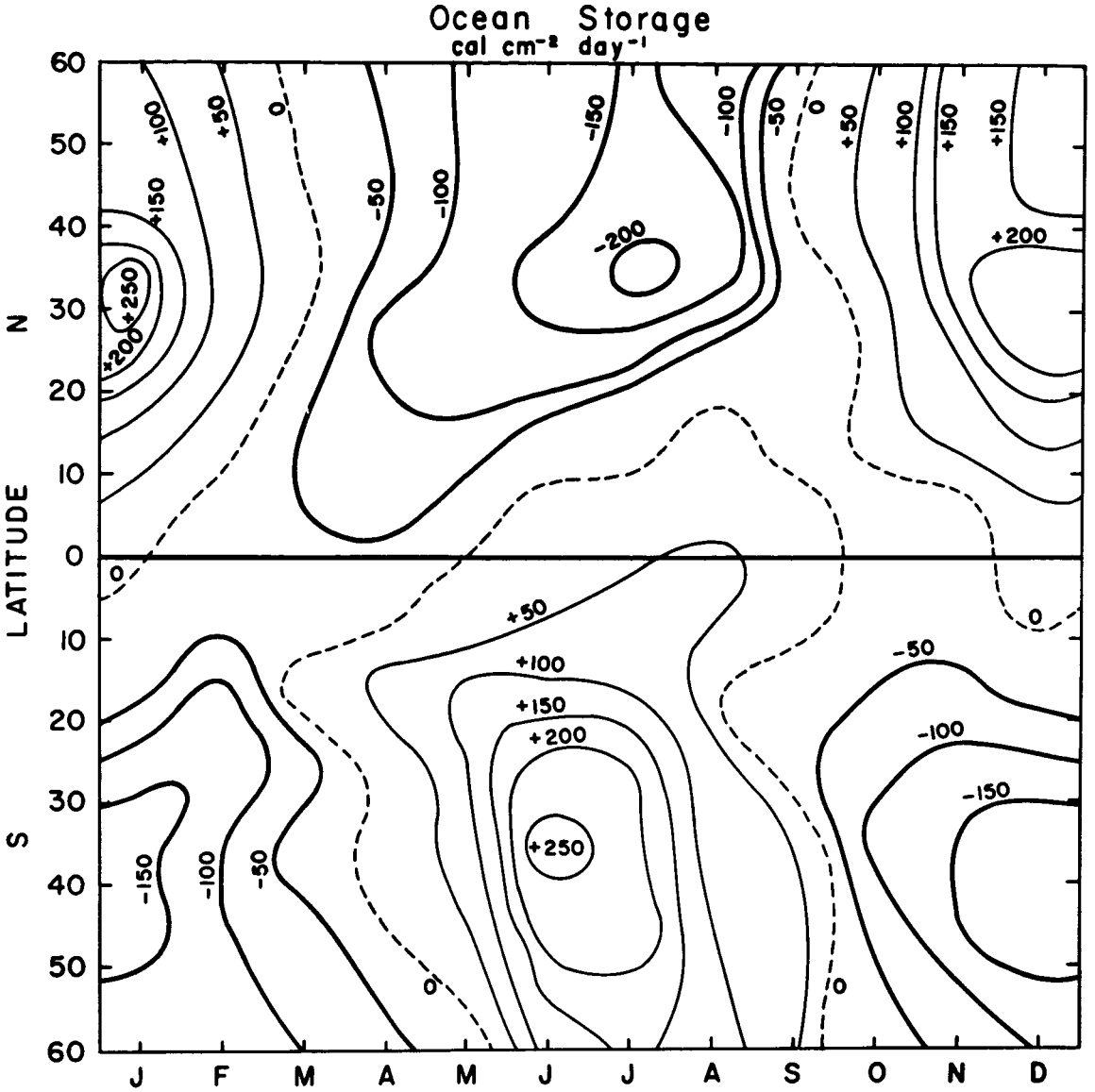

Figure 7. Latitude and time distribution of the storage of heat in the oceans in cal cm^{-2} day^{-1} ; (-) heat gained, (+) heat released.

4.2 Land

The storage in land has been estimated by Gabites. Because of the low heat capacity, the total heat storage in the land is very small, about 5 percent of that stored in the oceans. For our calculations, we therefore adopt the values given by Gabites.

4.3 Atmosphere

The heat storage in the atmosphere is also very small. Again Gabites has shown that on an average it is less than 10 percent of the total storage. These results are in agreement with the more recent findings of Davis (1963). We therefore adopt the values tabulated by Gabites for storage in the atmosphere.

5. Net latent heat

There is a significant amount of latent heat added to the atmosphere by water vapor when it condenses to form clouds. A large amount of heat is also used to evaporate water from the oceans and to some extent from the land. However, in any region, since the heat used up to evaporate water is not necessarily equal to the latent heat released by condensation, we get an imbalance of latent heat. This imbalance, called the net latent heat, is equal to 600 (P-E) cal, where P is the precipitation and E is the evaporation, expressed in cm and 600 cal gm^{-1} is the latent heat of water.

Estimates of the global distribution of evaporation on a seasonal basis have been made by several authors. The most comprehensive monthly charts for the oceans have been published in an atlas by Budyko

(1955). From these charts we have obtained the monthly mean evaporation over the oceans for each 10° latitudinal belt between 60°N and 60°S. The total evaporation from the oceans over the globe, according to Budyko (1955) is 1130 mm $year^{-1}$. Evaporation from the land, though considerably less, is not insignificant. Budyko (1956) gives an estimate of 450 mm $year^{-1}$ and has tabulated annual evaporation estimates for land for each 10° latitudinal belt. In order to evaluate the monthly variation of evaporation from land for each 10° latitudinal zone, we have adopted the following procedure:

Budyko (1955) has given monthly values of evaporation for several land stations scattered around the globe. We have averaged the trend of these monthly variations for the stations which fall in the same 10° latitudinal belt and assume this trend to be representative of the land areas within this belt. However, since in some latitude belts there are no stations, we have judiciously interpolated the evaporation values between latitudes. Monthly values of evaporation from land have then been tabulated for each latitudinal belt so that their annual sums are consistent with the values published by Budyko (1956).

The total evaporation from a given latitude is derived by weighting the evaporation from oceans and from land according to the proportion of each area in that latitudinal belt.

The average annual evaporation for the whole globe is 930 mm $year^{-1}$ (Budyko).*

*Recently Budyko (1963) has published a revised version of the Atlas of Radiation Balance in which global distribution of evaporation from both ocean and land is plotted for individual months. Also the average evaporation for the year is given as 1000 mm. These new values will change our evaluation of the net latent heat by a very small amount as we are interested in the monthly and latitudinal variation of the difference between evaporation and precipitation.

5.1 Precipitation

In order to conserve the total amount of water in the hydrosphere, the annual precipitation over the whole globe must equal the evaporation of 930 mm $year^{-1}$.

Brooks (1927) made a comprehensive study of the precipitation values over the globe and has given monthly means for every 5° latitudinal belt separately for ocean and land. He gave an annual estimate of 975 mm for precipitation over the whole globe. Extensive analysis of the rainfall over oceans has been made by Meinardus (1934), Wüst (1936), and, more recently, by Drozdov (1953). The values tabulated by Drozdov for oceans are consistently higher by 20 percent than those of Wüst (1936), but show the same distribution pattern. Wüst (1957) has recently given a revised estimate of the precipitation over oceans, but according to Malkus (1962), values given by Drozdov are more reliable. Drozdov's estimates agree better with those of Meinardus and therefore with those given by Brooks. We have therefore corrected the monthly mean values tabulated by Brooks to obtain a total annual precipitation of 930 mm $year^{-1}$ over the whole globe. A correction of 0.952 is applied to Brooks' rainfall data to obtain an agreement with Budyko's estimate of annual evaporation over the whole globe.

5.2 Net latent heat

The net latent heat deposited in the atmosphere is calculated by taking the difference between the amount of precipitation and evaporation for each month and for each latitudinal belt. In Figure 8 we show the distribution of net latent heat thus obtained in cal cm^{-2} day^{-1}. This

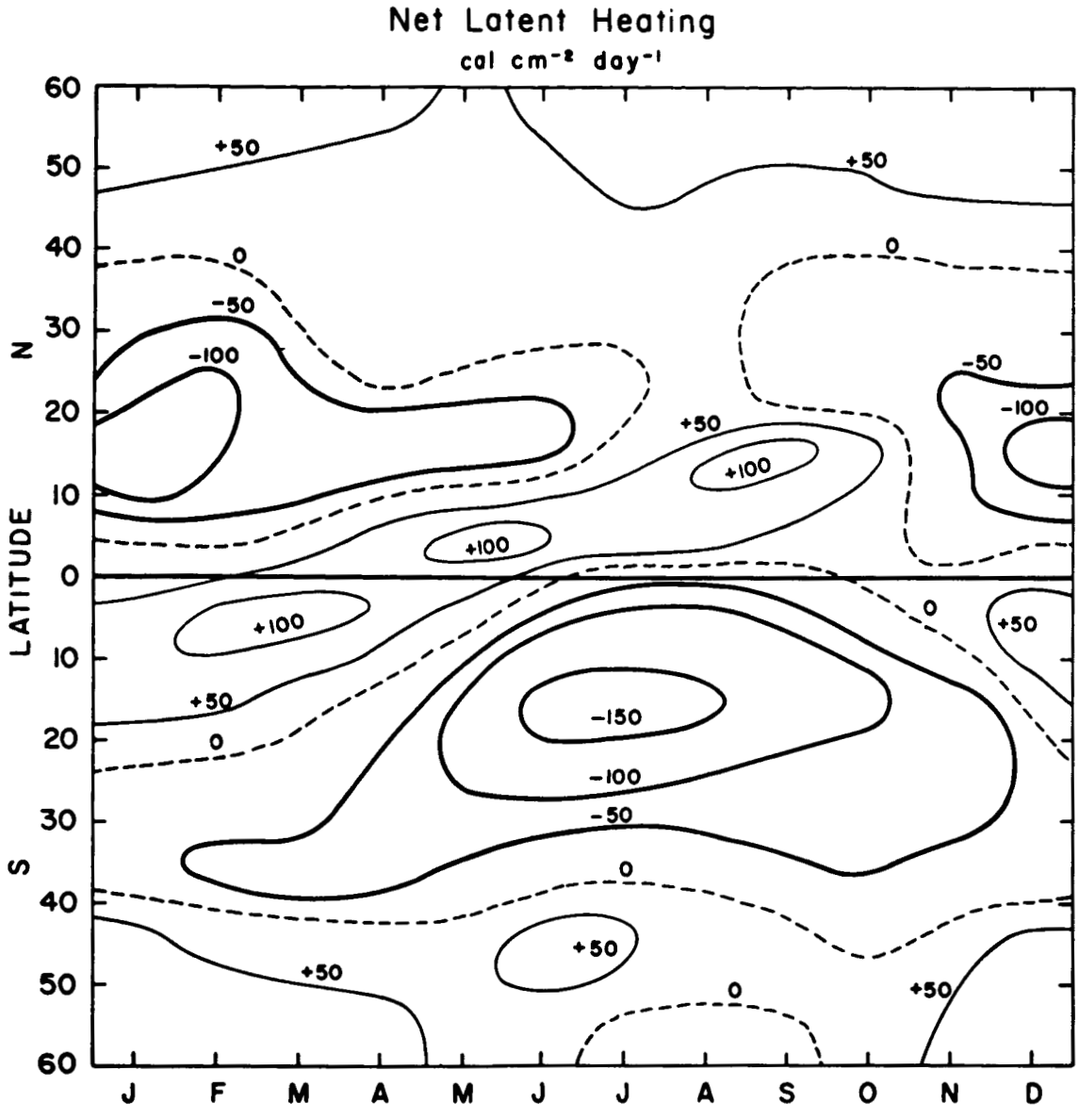

Figure 8. Latitude and time distribution of the net latent heat in the earth's atmosphere in cal cm^{-2} day^{-1}; (-) heat lost by the atmosphere because of evaporation over precipitation, (+) heat gained by the atmosphere by the excess of precipitation over evaporation.

figure shows the excess of precipitation over evaporation in the equatorial regions during most of the year. The subtropical belts, on the other hand, show an excess of evaporation throughout the year.

6. Net heat available for transport

The distribution of the net heat available for transport (NHAT), shown in Figure 9, is obtained by adding radiation balance, the storages and net latent heat. This heat is available for transport across the latitudinal circles by ocean currents and by winds. It seems difficult to comment on the accuracy of these quantitative estimates of NHAT. These numbers result from differences of the three large quantities which inherently have some errors due to the various assumptions made in their evaluation. It is, nevertheless, expected that the distribution of NHAT is physically meaningful and could be compared with some observed characteristics of the circulation in the atmosphere and oceans.

Figure 9 indicates a large excess of NHAT in the equatorial latitudes almost throughout the year. The reason for this is the positive radiation balance (Fig. 6) and positive net latent heat (Fig. 8), arising from an excess of precipitation over evaporation at these latitudes. The ocean storage (Fig. 7) in the equatorial regions is too small to influence the balance.

In February and March the maximum of this equatorial excess of NHAT occurs at 10°S, while in July and August, following the thermal equator, the maximum moves to 10°N.

In the subtropical latitudes, the radiation balance (Fig. 6) and net latent heat (Fig. 8) appear to vary in phase with each other, being

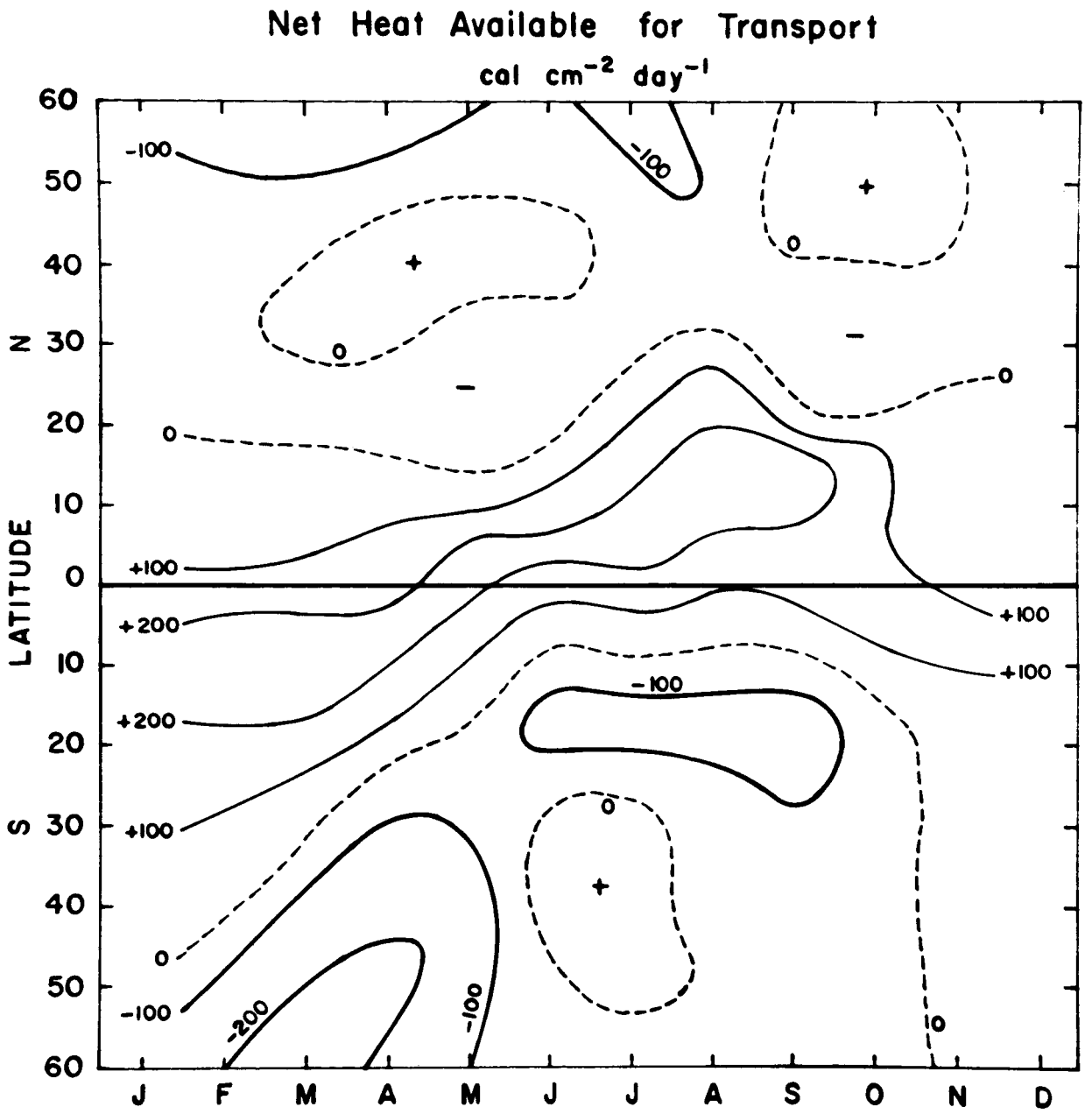

Figure 9. Latitude and time distribution of the net heat available for transport by the atmosphere and oceans across the latitude circles.

largest in summer and smallest in winter. On the other hand, the total heat storage in the oceans is equal in magnitude to the sum of radiation balance and the net latent heat but has an opposite phase. Consequently, in the subtropical latitudes, there is little energy available for transport through most of the year. In the case of the northern hemisphere, Fritz (1958) has already shown that between 20 and 40° latitudes the atmosphere may be in equilibrium throughout the year.

In the middle latitudes and toward the poles the energy balance is predominantly negative.

An examination of Figure 9 reveals a much stronger latitudinal gradient of the NHAT in the southern hemisphere as compared to the northern hemisphere. On an annual basis, Budyko (1956) has estimated that between 0 and 20°S as much as 80 percent of the energy may be transported southward by the oceans. Figure 9 indicates that, in the southern hemisphere, the ocean currents may be playing a major role in transporting heat across the latitudes. This appears to be the case especially in the months February, March, and April when the latitudinal gradient of NHAT is particularly large in the southern hemisphere.

References

Angström, A., 1963: Atmospheric turbidity, global illumination and planetary albedo of the Earth. Tellus, 14, 435.

Arking, A., 1964: Paper presented at the International Radiation Commission Symposium, Leningrad, U. S. S. R.

Astheimer, R. W., et al., 1961: Infrared radiometric instruments on Tiros II. J. Optical Soc. Amer., 51, 1386.

Bandeen, W. R., et al., 1961: Infrared and reflected solar radiation measurements from the Tiros II meteorological satellite. J. Geophys. Res., 65, 3165.

Brooks, C. E. P., 1927: Mean cloudiness over the Earth. Mem. Roy. Soc., 1, 127.

Budyko, M. I., 1955: Atlas of the heat balance. Leningrad.

Budyko, M. I., 1956: The heat balance of the earth's surface. Translated from the Russion edition by Nina A. Stepanova (U. S. Weather Bureau, Washington, D. C., 1958).

Budyko, M. I., 1963: Atlas of the heat balance of the earth. Leningrad.

Buettner, K. J. K., 1929: Meteor. Z., 46, 525.

Danjon, A., 1936: Novelles recherches sur la photométrie de la lumière cendrée et l'albedo de la terre. Ann. de l'Observatoire de Strasbourg, III, Fasc. 3.

Davis, P., 1963: An analysis of the atmospheric heat budget. J. Atm. Sci., 20, 5.

Drozdov, O. A., 1953: Annual amounts of precipitation. Marine Atlas, Vol. II, sheet 48B.

Dubief, J., 1959: Le climat du Sahara. Vol. I. Univ. d'Alger, Inst. Recherches Sahariennes, Alger.

Fritz, S., 1949: The albedo of the ground and atmosphere. Bull. Amer. Meteor. Soc., 29, 303.

Fritz, S., 1958: Seasonal heat storage in the ocean and heating of the atmosphere. Arch. Meteor., Geophy. Bioklimat., 10, 4.

Gabites, J. F., 1950: Seasonal variations in the atmospheric heat balance. Ph. D. thesis, Massachusetts Institute of Technology, Cambridge, Massachusetts.

Houghton, H. G., 1954: On the annual heat balance of the norther n hemisphere. J. Meteor., 11, 1.

House, F., 1964: Paper presented at the International Radiation Commission Symposium, Leningrad, U. S. S. R.

London, J., 1957: A study of the atmospheric heat balance. Final Report, Contract No. AF 19(122)-165, Research Division, College of Engineering, New York University, New York.

Malkus, J. S., 1962: Large-scale interactions. In The Sea, Hill, M. N., editor. John Wiley and Sons: New York.

Meinardus, W., 1934: Eine neue Niederschlagkarte der Erde. Petermanns geog. Mitt., 80, 1.

Nordberg, W., et al., 1962: Preliminary results or radiation measurements from the Tiros III meteorological satellite. J. Atm. Sci., 19, 20.

Prabhakara, C., and Rasool, S. I., 1963: Evaluation of Tiros infrared data. In Rocket and Satellite Meteorology, Wexler, H. and Caskey, J. E. Jr., editors. North-Holland Publishing Company: Amsterdam.

Rasool, S. I., 1964: Global distribution of the net energy balance of the atmosphere from Tiros radiation data. Science, 143, 567.

Shroeder, E., and Bryan, K., 1960: Seasonal heat storage in the northern hemisphere. J. Meteor., 17, 670.

Simpson, G. C., 1929: The distribution of terrestrial radiation. Mem. Roy. Met. Soc., 3, 53.

Suomi, V. E., 1958: Ann. of I. G. Y., Vol. 6.

Suomi, V. E., 1961: Earth's thermal radiation balance, preliminary results from Explorer VII. I. G. Y. Bull., 52.

U. S. Navy, Chief of Naval Operations, 1955: Marine climatic atlas of the world.

Wüst, G., 1936: Oberflächensalzgehalt, Verdunstung, und Niederschlag auf dem Weltmeere. Landes. Forsch. Festschr. Norbert Krebs., 347.

Wüst, G., 1957: Stromgeschwindigkeiten und Strommengen in den Tiefen des Atlantischen Ozeans. Wiss. Ergebn. Deut. Atlant. Exped. 'Meteor', 1925-1927. Band VI, Teil 2. Walter de Gruyter and Co.: Berlin.

Winston, J. S., and Rao, P. K., 1962: Preliminary study of planetary-scale outgoing longwave radiation as derived from Tiros II measurements. Mon. Wea. Rev., 90, 307.